Smartphone behavior is suppressed during bursts of wake slow waves

Ruchella Kock[1,*], David Hof[1], Reto Huber[2,3], and Arko Ghosh[1,*]

[1] *Cognitive Psychology Unit, Institute of Psychology, Leiden University, The Netherlands*

[2] *University Children's Hospital, University of Zurich, Switzerland*

[3] *Department of Child and Adolescent Psychiatry and Psychotherapy, Psychiatric Hospital, University of Zurich, Switzerland*

[*] *Corresponding author(s): Leiden University, Wassenaarseweg 52, Leiden, 2333 AK, a.ghosh@fsw.leidenuniv.nl [Arko Ghosh], r.m.d.kock@fsw.leidenuniv.nl [Ruchella Kock]*

Abstract

Real-world behavior unfolds as a continuous flow of actions over time. One possibility is that this continuous flow is enabled by a seamless stream of cortical activity. However, emerging evidence suggests that even during ongoing behaviors, cortical neural populations undergo brief periods of silence. This 'off-state' can be detected as wake slow waves in EEG, similar to the slow waves characterizing deep sleep. Here, we leveraged the spontaneously occurring fluctuations in smartphone touchscreen interactions in combination with EEG to investigate the dynamics of slow waves during behavior. We report that wake slow waves occur more frequently during a session of smartphone behavior than during a session of prolonged rest (∼1 h). We find that slow waves can occur in bursts - characterized by short consecutive intervals - interleaved with longer periods of absent slow waves. During smartphone use, the probability of bursts increased compared to rest, and the duration of burst-absent periods decreased. During the bursts, however, the likelihood of generating smartphone interactions was substantially diminished. Conversely, the periods of absent slow waves were more permissive to the behavioral output. We speculate that the dynamics of neural silencing are configured according to the overall behavioral state. This configuration, in turn, allows behavioral outputs to leverage the windows of opportunity that emerge between slow wave bursts. Our study, combining smartphone behavior with EEG, reveals how brief cortical silencing events punctuate the seemingly continuous flow of everyday actions.

Author contributions

A.G. conceived the study. R.K., D.H., and A.G. designed the study. R.K. and D.H. analyzed

the data aided by A.G. A.G. drafted the report aided by all authors. R.H. contributed with the methods for slow wave detection. All authors helped edit the manuscript.

Acknowledgments

The authors would like to thank the student assistants who contributed to the data collection at Leiden University. The authors would like to thank Steven Militec for his feedback regarding the statistical analysis.

Funding

This study was funded by a research grant from Velux Stiftung (no. 1283, awarded to A.G.).

Competing interests

The authors declare the following financial interests/personal relationships which may be considered as potential competing interests: Author R.K. is co-founder of Axite BV, Leiden, The Netherlands. Axite creates software for remote monitoring of brain functions by linking consumer-grade EEG and smartphone behavior. A.G. is co-founder of QuantActions AG, Zurich, Switzerland. QuantActions converts smartphone interactions into brain health metrics. The smartphone data collection for this study was performed using QuantActions software and services. This study is linked to a patent filed by A.G., who is the scientific advisor of Axite. Authors D.H. and R.H. have no conflicts to declare.

1 Introduction

In our daily lives, we generate a seemingly continuous flow of actions. It is generally held that to enable this flow, cortical activity may seamlessly continue without any breaks [Histed et al., 2009, Huk et al., 2018]. For instance, according to invasive recordings in non-human primates, prefrontal cortical activity can seamlessly persist from one task to the next, and the cortical preparation for the subsequent tasks can begin well before the completion of the current task [Histed et al., 2009]. However, there is a parallel body of work in sleep research, which indicates that cortical neurons can undergo periods of silence (off-state) followed by high neural firing (on-state) [Steriade et al., 1993]. In theory, these off-states can break the continuous stream of cortical processing and disconnect cortical networks [Massimini et al., 2005]. While these off-states are a defining feature of deep sleep, growing evidence shows that they can also occur during wakefulness, albeit more localized than in sleep [Bernardi et al., 2015, Vyazovskiy et al., 2011, Nir et al., 2017, Hung et al., 2013]. In EEG recordings, these cortical off-states are captured as large-amplitude slow waves in the delta (1–4 Hz) or theta (4–7 Hz) range [Sachdev et al., 2015, Andrillon et al., 2021]. Although the occurrence of wake slow waves

is increasingly studied for isolated behavioral tasks [Andrillon et al., 2021], how they unfold when engaged in the flow of real-world activities remains unknown.

The ubiquitous use of smartphones offers a fresh opportunity to study the links between wake slow waves and behavior. Emerging evidence suggests that cortical activity tracks moment-to-moment fluctuations in smartphone touchscreen interaction dynamics [Wan and Ghosh, 2025]. For instance, the frontal cortical oscillations in the theta range are more pronounced during frequent vs. infrequent touchscreen interactions [van de Ruit and Ghosh, 2022]. In people with epilepsy, epileptiform discharges (bursts of abnormal neural activity) are correlated to smartphone touchscreen interaction dynamics, albeit the links are not simply linear [Duckrow et al., 2021]. The more pronounced disruptions (i.e., seizures) also leave a fleeting mark in smartphone touchscreen dynamics [van Nieuw Amerongen et al., 2024]. These scattered observations raise the possibility that the distribution of transient cortical off-states, too, may be linked to the behavioral fluctuations captured on the smartphone touchscreen.

According to a conventional idea, the distributions of wake slow waves are simply governed by a slow drift (on the scale of hours). Essentially, the density of wake slow waves may increase as a function of time spent awake, as found for slow wave activity during sleep [Borbély et al., 1982]. Supporting this idea, sleep deprivation studies show that wake slow waves become more frequent and higher in amplitude as the time spent awake is experimentally increased [Finelli et al., 2000, Snipes et al., 2023]. A parallel body of work on both wake and sleep states suggests that the distribution of slow waves is not simply governed by time awake, but also by the extent of cognitive demand, recent experiences, and area-specific plasticity processes [Halász et al., 2014, Huber et al., 2004, Huber et al., 2006, Snipes et al., 2022, Hung et al., 2013, Massimini et al., 2005, Quercia et al., 2018, Pinggal et al., 2022]. Smartphones engage a range of cognitive processes and contribute to experience-dependent plasticity, further raising the possibility that slow waves may be linked to the rich behaviors captured on the smartphone [Balerna and Ghosh, 2018, Gindrat et al., 2015, Ceolini et al., 2022].

An alternative putative link between slow waves and behavior is driven by the idea that intervals between wake slow waves may indicate cortical states that are more or less conducive to behavior. This idea stems from the observation that in cortical stimulation studies, which interrupt ongoing neural activity, the intervals between stimulations influence the nature of the outcome [Cash et al., 2010, Benali et al., 2011, Ferreri et al., 2011, Bolognini and Ro, 2010]. The link between stimulation intervals and the outcome is not simply linear, as behavioral effects can be visible only in a certain range of intervals [Luber et al., 2007]. Moreover, depending on the stimulation interval, the induced interruptions can counterintuitively induce performance improvement in some tasks [Luber and Lisanby, 2014]. Although the interval statistics of wake slow waves are not clear, the tem-

poral distribution of sleep slow waves shows meaningful nonlinear fluctuations within a single night [Wei et al., 2020, Chauvette et al., 2011].

To probe the putative importance of the temporal distribution of slow waves, they can be separated according to the interval dynamics while addressing their link to smartphone behavior. Towards this, a train of slow waves can be separated using a joint-interval distribution (JID). Essentially, the interval between two consecutive wake slow waves (K) can be considered along with the next interval ($K+1$). These intervals can then be pooled in two-dimensional bins by calculating the joint distribution. These bins capture the probability of slow waves, separating rapid (say 300 ms) from sparse consecutive slow waves (say 30 s). The JID has been extensively used to separate the temporally diverse neural, cardiac, and behavioral activity, and here we extend it to the study of slow waves [Brennan et al., 2002, Rodieck et al., 1962, Eagan and Partridge, 1989, Ceolini and Ghosh, 2023, Duckrow et al., 2021].

We investigated the distribution of slow waves during ongoing smartphone interactions in 60-minute-long behavioral sessions. First, we compared the appearance of slow waves captured during the behavioral session to a similar period of restful movie watching [Meer et al., 2020, Espenhahn et al., 2020]. Next, we examined how the temporal dynamics of slow waves differed between the two sessions. Finally, using high-resolution smartphone touchscreen logs, we found that behavioral activity was reduced during periods when slow waves occurred in close succession, that is, in bursts. These findings suggest that the temporal dynamics of slow waves reflect underlying cortical patterns that align with fluctuations in real-world behavior.

2 Results

Slow waves in smartphone behavioral session and rest

We captured slow waves by using EEG during a session of restful movie watching (∼60 minutes) followed by a session of smartphone use (∼60 minutes). The recording sessions were distributed between morning to late afternoon, with session onset times ranging from 7 am to 5 pm (Supplementary Figure 1). We also kept track of the putative amount of sleep throughout the week prior to the measurement (Supplementary Figure 2). A substantial increase in slow waves driven by sleep pressure is not expected within the 1-h smartphone and 1-h rest observation period. To test this, we fitted a linear regression model predicting the number of slow waves (slow wave density estimated within 1-min time windows) from session type (movie vs. smartphone), time elapsed within session, and their interaction (Supplementary Figure 3). Neither time elapsed nor the interaction term reached statistical significance (all $p > 0.05$ after multiple comparison correction; MCC). Session type, however, was

significantly associated with slow wave density (see below for equivalent results of the direct comparison of slow wave density between sessions). These findings indicate that the number of slow waves did not substantially increase linearly with time.

We compared slow waves recorded during the smartphone use session with those observed during rest. For this comparison, we quantified three key features of slow waves: (i) density (frequency of neural silencing), (ii) amplitude (extent of neural synchrony), and (iii) upwards and downwards slopes (indices of synaptic strength, with steeper slopes reflecting stronger synapses [Jaramillo et al., 2020]). Slow waves were present across the scalp in both sessions. During smartphone behavior, the density of slow waves was higher compared to rest (Figure 1, paired t-test). Higher slow wave density was observed across most regions of the scalp, except for parieto-occipital areas. In contrast to the density, amplitudes were marginally reduced during smartphone behavior at frontal and temporal sites, but remained unchanged at parieto-occipital electrodes. During smartphone behavior, the slopes were marginally shallower than at rest across the scalp, except for central and occipital regions, where they were slightly steeper. In sum, slow wave density, amplitude, and slope all varied between sessions, with most differences spanning the scalp, with the exception of parietal/occipital electrodes. Given the high similarities between slow wave amplitudes and slopes, we did not consider the slopes in subsequent analyses.

We note that the restful session showed slow wave topography in keeping with what has been observed before [Andrillon et al., 2021]. The central electrodes showed the highest density compared to the rest of the scalp. The amplitudes remained the largest in the frontal electrodes compared to the rest of the scalp. Finally, the slopes were the shallowest in the sensorimotor areas. Furthermore, as smartphone interactions may evoke event-related potentials, there may be a methodological concern that this evoked activity is mistaken for slow waves. However, this is rather unlikely given that they were also observed at rest. Furthermore, in our previous work that captured the smartphone touchscreen-related ERP (smERP), the ERP amplitudes were smaller than those for slow waves by a magnitude (1 μV for ERP vs. 10 μV for slow waves). Finally, the smERP is concentrated over the contralateral sensorimotor cortex, whereas the slow waves were detected across the scalp and bilaterally [Kock et al., 2023].

Coarse-grained links between slow waves and fluctuations in smartphone interactions

A previously used approach to study the links between EEG oscillations and smartphone behavior is to quantify EEG and behavioral parameters in 1-minute bins followed by a regression analysis [van de Ruit and Ghosh, 2022]. This approach offers a tangible first step to study the simple linear

links between slow waves and behavior. Towards this, we computed the slow wave density and median amplitudes and correlated these with the number of smartphone interactions occurring in the same bins. First, we performed simple pairwise Spearman correlations between the behavior and slow wave density and amplitudes (Supplementary Figure 4). No reproducible statistically significant correlations were observed after multiple comparison correction. Although a few isolated electrodes reached significance in 7 of 47 participants, these effects were spatially sparse and not reproducible across individuals. Next, we conducted a hierarchical mass-univariate (multi-variate regression) analysis across all electrodes to explain the variations in behavior using both slow wave features. We found significant clusters over the frontotemporal and sensorimotor regions where an increase in slow wave density was accompanied by a decrease in the number of smartphone interactions (Supplementary Figure 4). However, the slow wave amplitude did not reveal significant clusters. These coarse-grained patterns indicate that the slow wave density, when adjusted for the variance in amplitude, is loosely linked to smartphone behavioral fluctuations.

Fine-grained dynamics of slow waves in smartphone behavioral session and rest

To study the fine-grained temporal dynamics of slow waves, we focused on the intervals between consecutive events. Specifically, we captured the probability of a given interval (K) occurring together with the following interval (K+1) using a joint-interval distribution (JID; Figure 2, Supplementary Figure 5). Here, we report on two sets of analyses using these distributions collected during the smartphone use and rest sessions. The first analysis used data-driven dimensionality reduction to reveal the typical dynamics of slow waves distributed across the scalp in the two types of sessions. The second analysis compared the distributions using paired t-tests.

First, to identify the typical slow wave patterns distributed across electrodes, we applied non-negative matrix factorization (NNMF). This dimensionality reduction technique reduced the high-dimensional JID $\times$ electrode tensor into vector pairs. Each resulting pair indicated a pattern of prototypical slow wave intervals (meta-JID) and its spatial distribution across electrodes (meta-location). For each individual, this reduction typically revealed two distinct prototypical JIDs, regardless of session type (rest or smartphone behavior). Clustering these patterns at the population level revealed two dominant classes at rest: (i) sparse consecutive slow waves, occurring primarily at central, parietal, and occipital electrodes, and (ii) rapid consecutive slow waves (i.e., bursts), largely absent from those regions but prevalent at frontal electrodes. During smartphone behavior, four common classes emerged: (i) a pattern similar to that seen at rest, with sparse consecutive slow waves across central, parietal, and occipital electrodes; (ii) rapid consecutive slow waves, less prominent over central

electrodes and more irregularly distributed across the scalp; (iii) rapid consecutive slow waves (faster than pattern 'i' but slower than 'ii'), mainly at frontal sites; and (iv) sparse consecutive slow waves localized to occipital electrodes. These patterns indicate that, while there may be slow wave dynamics common to both rest and smartphone behavior, smartphone behavior may engage an additional set of dynamics spanning the frontal and occipital electrodes.

Second, we performed mass univariate paired t-tests spanning the scalp electrodes and the two-dimensional bins of the JID to compare the slow wave probability between rest and smartphone behavior (Figure 3 and Supplementary Figure 6). This analysis revealed a higher probability of slow wave bursts during smartphone behavior compared to rest, and a lower probability of sparse consecutive intervals during the behavior. Statistically significant JID clusters were observed across the scalp, except at the occipital electrodes. According to the NNMF patterns reported above, the rapid vs. slow dynamics were distinctly distributed across the scalp. The mass univariate pattern further adds to the distinction between the rapid and sparse slow wave dynamics.

Rapid slow wave dynamics are not permissive to smartphone behavior

According to both the coarse-grained and fine-grained analyses, slow wave dynamics were linked to smartphone behavior. Given the distinct pattern of results for the rapid vs. sparse consecutive slow waves, we next report on the nature of the behavioral output during these different dynamics. Towards this, we estimated the rate of smartphone interactions as a function of the slow wave dynamics captured using the JID, at each electrode. The rate was defined as the number of smartphone interactions during consecutive slow wave intervals (K to K+1), divided by the duration of those intervals. We averaged across the population to focus on the consistent patterns (Figure 4, Supplementary Figure 7). We consistently observed a scalp-wide pattern: the rate of smartphone interactions was lowest ($\sim$0) during rapid consecutive intervals, and the rate gradually increased along the JID diagonal, with slow consecutive intervals showing the highest rates. We next addressed the latency to smartphone interactions after the slow wave, as a function of the JID (Supplementary Figure 8). We found a marginal gradient: the latency was longest ($\sim$54 s) following rapid consecutive slow waves, and gradually shortened ($\sim$1 s) as slow waves became sparser. These findings suggest a brain-wide coupling between slow wave dynamics and both the immediate and the future smartphone interactions.

Finally, in the fine-grained analysis presented above, we separated the slow wave features according to their interval dynamics. It is possible that slow wave features co-vary with the dynamics. We focused on two features: the amplitude of the slow wave (Supplementary Figure 9) and the duration of the slow wave (Supplementary Figure 10). The population averaged (median) amplitudes varied along the diagonal of the JID: rapid consecutive slow waves were associated with larger amplitudes relative to

the sparser (slow consecutive) slow waves. This pattern was visible across the scalp. The slow wave duration (median) also varied along the diagonal of the JID, with shorter slow waves during rapid intervals (∼500 ms). In sum, slow vs. rapid consecutive slow waves distinctly reflect neural features and behavioral output.

3 Discussion

We observed wake slow waves during both active smartphone use and restful movie watching. In a coarse-grained analysis of wake slow waves, we simply estimated their temporal density, and in a fine-grained analysis, we quantified their interval dynamics. Both of these analyses showed that the temporal distribution of slow waves differs between the two sessions. The density of slow waves was higher in the smartphone use session. The fine-grained analysis revealed a spectrum of slow wave dynamics, from rapid consecutive intervals (i.e., bursts) to sparse periods of slow waves. Smartphone touchscreen interactions were the least likely to occur during the bursts, although the bursts themselves were more likely in the smartphone use session compared to rest. These patterns suggest a configuration of slow waves at different time-scales, where the overall behavioral state (smartphone use vs. rest) dictates the dynamics of neural silencing. The resulting pattern of intermittent, brief silencing may organize or gate behavioral output, with the periods absent of slow wave bursts serving as windows of opportunity for action.

The temporal distribution of slow waves and their behavioral correlates indicate that wake slow waves do not simply reflect a monotonic accumulation of sleep pressure within the hour-long recordings. First, there was not a simple linear drift in the minute-by-minute slow wave density estimates within the restful or smartphone recording sessions. Second, in either of the two sessions, the slow wave interval dynamics captured in the JID did not reveal signatures of a simple drift, such as a long interval being consistently followed by a shorter interval. Third, within the smartphone use session, slow waves were correlated to the non-linear behavioral fluctuations. While sleep pressure may still accumulate through the course of a full day, our findings support the notion that, at shorter timescales ($\sim$ 1 h), wake slow waves are more closely linked to ongoing behavioral fluctuations than being attributable to a gradual buildup throughout the day. Still, the behavioral correlates of sparse wake slow waves we discovered here were in individuals who were rather well rested, and whether the links are sustained under high sleep pressure will need to be addressed next.

Wake slow wave dynamics were closely linked to the overall behavioral state. There was an increase in the density of slow waves during the smartphone use session, which was further clarified by our interval analysis as an increase in slow wave bursts and a reduction in periods of slow

wave absence. A minute-by-minute analysis revealed a positive correlation between the number of touchscreen interactions and slow wave density, suggesting that the wake slow wave configuration is continuously updated. This dynamic configuration likely involves coordinated changes across cortical areas, as evidenced by a higher slow wave density in the frontotemporal and sensorimotor regions during the active behavioral state compared to rest. The slow waves in these regions also appeared to be more localized, as inferred from their smaller amplitudes during the behavior. This finding - specifically, the increased density of wake slow waves during behavior - appears to contrast with the emerging notion that these waves impair cognitive function and increase performance lapses [Bernardi et al., 2015, Nir et al., 2017, Andrillon et al., 2021]. This paradox raises the possibility that two distinct processes govern the behavioral correlates of slow waves: one where slow waves are re-configured in response to an altered behavioral state, and another where a slow wave transiently interrupts behavioral output. It remains unclear whether this overall behavioral configuration of localized and high-density slow waves is selectively driven by a specific factor, such as synaptic excitability, or if it emerges from the complex network activity underlying smartphone interactions [Vyazovskiy and Harris, 2013].

Our results strongly suggest that the influence of slow waves on behavioral output, i.e., the rate of touchscreen touches, is governed by slow wave interval dynamics. While touchscreen interactions were dampened during slow wave bursts (short consecutive intervals), the outputs were more likely to occur during longer periods of slow wave absence. This dynamic may also govern the extent of neural silencing, as bursts exhibited larger amplitudes than the isolated slow waves. This suggests that fluctuating opportunities for behavioral output are mediated by the temporal spacing of slow waves. The behaviorally constraining neural silencing may linger for a period after the slow wave, but only in the case of bursts, as indicated by the longer latencies to a touchscreen interaction. Given that bursts were interleaved by long periods of slow wave absence at rest, these slow wave absence periods may reflect a general opportunity for network processing; even in the absence of behavior [Hinard et al., 2012, Krueger and Roy, 2016].

In general, the functional role of wake slow waves, beyond the momentary disruption of behavioral output, remains unclear [Massimini et al., 2024]. One possibility is that these slow waves locally enhance responsiveness to incoming stimuli [Crochet et al., 2005, Vyazovskiy et al., 2013]. So, the bursts may be used to support dedicated periods of high sensitivity to incoming information, while slow wave absences are utilized for more intrinsic or top-down processes that enable behavioral output. When on the smartphone, the active engagement with tactile and visual information may require longer periods sensitive to external information than at rest, explaining the higher likelihood of the bursts. A range of functions have been associated with sleep slow waves, as in restorative benefits, includ-

ing synaptic homeostasis [Tononi and Cirelli, 2006], metabolic waste clearance [Xie et al., 2013], and memory consolidation [Diekelmann and Born, 2010]. However, the time constants underlying these various functions are out of reach of our hour-long recording sessions.

In conclusion, transient periods of neural silencing are a common feature that punctuate the apparently continuous flow of smartphone interactions. These silent periods, which occur with a range of interval dynamics, appear to form smartphone behavioral links according to these dynamics. This observation inspires ideas, such as a system that "flips" between periods sensitive to external information (supported by the bursts) and periods of top-down computation (during long periods of slow wave absences). This raises a critical question: how is the continuous flow of behavior sustained despite these moments of neural silencing? A delicate balance, potentially involving distributed neural networks, parallel processing, and memory, may help bridge these silent periods. This balance may be particularly fragile after sleep loss, when increased sleep pressure can tip the system into devastating bouts of neural silence, leading to a rise in human error [Nir et al., 2017]. While sleep slow waves are a well-established area of research focused on understanding how we sleep, our approach offers a new direction for unraveling how wake slow waves contribute to real-world behavior.

4 Methods

Participants and study design

Fifty-two (52) healthy participants ranging between 23 to 52 years old (median = 29) were recruited on Leiden University campus through flyer-based advertisements. The inclusion criteria included only right-handed individuals (self-report). During the study, the participants installed an app that collected their smartphone behavioral datasets (described below) at least one week prior to the measurement. Participants came to the Leiden University campus for EEG measurements, where they first watched a movie (David Attenborough, Africa, 2013) for ∼60 minutes, followed by a period of ∼60 minutes where they interacted with their smartphone (see Supplementary Figure 1 for the duration of the sessions). Participants were instructed to use their right thumb on the smartphone, which we validated via live video streaming. Throughout the measurement, participants were encouraged to take breaks when needed. A subset of the participants (14) performed two separate sessions with identical study procedures, conducted approximately one week apart, as part of a larger project. The measurement with the longest smartphone recording was selected for analysis. Due to a technical error, 6 participants had less than 15 minutes of smartphone data and were excluded from further analyses. The final analyses were conducted with a sample size of 46 (19 female, 20 male, 7 participants' gender and age data were not available).

Ethics

The study proposal was approved by Leiden University Psychology Research Ethics Committee, Leiden, The Netherlands (Number: V1-920) on 07-04-2020. The proposal was titled: 'Unravelling brain plasticity through smartphone interactions'. Before the study, the participants signed a written informed consent form, and at the end of the study, they were debriefed about the study goals.

Smartphone data collection

Smartphone behavior was collected with an app called TapCounter (QuantActions AG, Zurich), which collects (i) the timestamp of touchscreen interactions on the smartphone, (ii) the active app, and (iii) the screen lock and unlock times. The app operated in the background while participants were using their smartphones freely. The timestamps were collected at millisecond resolution (mean error = 0, standard deviation = 15 milliseconds) [Balerna and Ghosh, 2018]. Throughout the measurement, the participant used their top 2 social and top 2 non-social apps, switching every 10 minutes between apps. The top apps were selected based on high usage in the two weeks leading up to the measurement. Beyond these app selections, participants could use their smartphones freely without any additional instructions. To account for potential outliers introduced by a break (∼5 minutes) during the recording, we removed the EEG data between the largest gap in behavioral interactions for each participant.

Putative sleep detection

Putative sleep duration was estimated based on smartphone usage patterns, as smartphones are often the first and last devices used each day (e.g., to set or turn off an alarm). The durations were calculated by subtracting the timestamp of the last interaction on the previous night from the timestamp of the first interaction on the following morning. We estimated sleep duration for the night preceding the experiment, as well as the median sleep duration across the seven nights prior to the experiment. This method of estimating sleep duration has been validated previously and contrasted to sleep durations collected through wearable devices [Borger et al., 2019, Massar et al., 2021].

EEG data collection, processing, and slow wave identification

EEG data were collected while participants were watching a movie or using their smartphone in a Faraday cage. The Faraday still enabled WIFI connectivity or access to mobile networks. The collection was performed using a 64-channel EEG cap and the BrainAmp 64-channel DC amplifier by Brain Products (GmbH Gilching). The data was collected at a 1000 Hz resolution.

We preprocessed the EEG data offline using MATLAB 2023b (MathWorks, Natick) and EEGLAB

[Delorme and Makeig, 2004]. The preprocessing pipeline for slow wave detection included several steps. First, channels with high impedance (larger than 10 kΩ) were identified and replaced with interpolated data. Blink-related artifacts were removed using Independent Component Analysis (Infomax), and the two ocular electrodes were excluded from all subsequent analyses. The data were then band-pass filtered between 0.5 and 48 Hz, followed by downsampling to 128 Hz. We re-referenced the data to the average of all electrodes and subsequently to the left and right mastoid electrodes. A low-pass filter up to 4 Hz was then applied to isolate activity within the delta frequency band. Candidate slow waves were identified based on negative half-waves with durations between 0.1 and 1 s. Waves with positive peaks > 75 μV or occurring within 1 s of a large-amplitude event (absolute amplitude > 150 μV) were discarded. Finally, the 10% of waves with the largest peak-to-peak amplitudes per channel were selected for analysis. These steps follow established procedures for sleep slow wave detection [Riedner et al., 2007, Bernardi et al., 2015] and are based on an algorithm adapted for wake slow waves [Andrillon et al., 2021].

After identifying slow waves, we estimated three key features: (i) density, defined as the number of slow waves per minute; (ii) their mean absolute peak-to-peak amplitude; and (iii) their mean downward and upward slopes, calculated as the average change in voltage per second between the start of the wave and the negative peak, and the negative peak and the positive peak, respectively.

Statistical analysis of slow waves and time elapsed

To test whether slow wave density increased as a function of time elapsed, we fitted a hierarchical linear regression model predicting the number of slow waves within a 1-minute time window from (i) session type (restful movie watching vs. smartphone use), (ii) time elapsed within restful movie watching and smartphone use session (in min; mean-centered per session), and (iii) their interaction. This allowed us to capture both an overall shift in slow wave density between sessions as well as session-specific time-related changes in slow waves. At the first level, the model was fitted separately for each participant and electrode. At the second level, we tested the β coefficients across participants using mass-univariate one-sample t-tests with multiple comparison correction in the form of cluster-based permutation testing ($\alpha = 0.05$; 1000 randomizations). We repeated this procedure for a reduced model without the interaction term to test for session-invariant time-related changes in slow wave density.

Statistical comparison of slow wave across rest and smartphone behavior

To compare slow waves between restful movie watching and smartphone behavior, we performed a series of mass-univariate (channel-wise) paired t-tests for slow wave density, amplitude, and slopes. Subsequently, we performed multiple comparison correction using cluster-based permutation testing ($\alpha = 0.05$; 1000 randomizations).

Coarse-grained relationship between slow waves and smartphone interactions

We assessed the relationship between slow wave features and the number of smartphone interactions using two approaches. Note, given the high correlation between amplitudes and upward/downward slopes, we did not include the slopes in any subsequent analysis. First, we computed the slow wave density and median amplitudes within 1-minute time bins, and correlated them with smartphone interaction counts from the corresponding time windows using Spearman's ρ. The correlations were computed for each individual at each electrode, and their significance was assessed via permutation testing in MATLAB. To correct for multiple comparisons, we used the False Discovery Rate (FDR) method with the Benjamini–Yekutieli adjustment ($\alpha = 0.05$) [Benjamini and Yekutieli, 2001]. However, this correlational approach treated each slow wave feature independently and therefore did not assess how the combination of features relates to smartphone behavior. Therefore, we then performed time-binned mass-univariate regressions to predict the number of smartphone interactions from slow wave features. The interaction count of each 1-minute window was predicted using slow wave density and median peak-to-peak amplitude from the corresponding 1-minute window. The regressions were conducted at the individual level for each electrode (LIMO-EEG Level 1 analysis). At the group level, we performed one-sample t-tests on the resulting β coefficients (LIMO-EEG Level 2 analysis). To correct for multiple comparisons across electrodes and participants, we applied spatiotemporal clustering (as implemented in LIMO) with 1000 bootstraps and a significance threshold of $\alpha = 0.05$.

Fine-grained relationship between slow waves and smartphone interactions Next, we examined the fine-grained relationship between slow waves and smartphone interactions by analyzing their interval dynamics using the joint-interval distribution (JID). The JID estimates the joint probability of observing two consecutive intervals between slow wave off-states: interval K and the following interval K+1. Off-states were defined as the largest negative peaks in the signal. Each interval pair (K and K+1) was assigned to a bin in a 2D matrix, and kernel density estimation was used to estimate the joint probability distribution over these bins. The JIDs were computed separately for each participant, session (restful movie watching and smartphone use), and electrode.

We used non-negative matrix factorization (NNMF) to extract prototypical patterns of slow wave dynamics across the scalp. NNMF is an interpretable dimensionality reduction technique that decomposes a matrix into low-rank representations. To determine the optimal number of representations (ranks) for each participant, we performed cross-validation by: (i) randomly masking 20% of the matrix, (ii) running NNMF 50 times for ranks 1–10 with random initializations, (iii) reconstructing the original matrix from the NNMF output, and (iv) selecting the rank with the lowest average recon-

struction error.

Since NNMF is non-convex and may produce different solutions across runs, we selected a stable solution by using the stable and reproducible NNMF (STAR-NNMF) method, as developed by [Ceolini and Ghosh, 2023]. STAR-NNMF involved running 1000 NNMF repetitions and selecting the decomposition with the highest median pairwise cross-correlation across runs. This process yielded, for each participant, prototypical JIDs (meta-JIDs) and their corresponding spatial distributions across the scalp (meta-locations), indicating where these patterns were most prominent. STAR-NNMF was performed separately for each participant and session.

At the group level, we clustered the meta-JIDs using k-means to identify population-wide patterns. We selected the optimal number of clusters (between 1 to 10) by using the Silhouette method, which measures the similarity within and between clusters. Since K-means is also a non-convex algorithm, we performed 1000 repetitions with randomly initialized values and selected the repetition with the smallest sum of squared distances [Lisboa et al., 2013].

To statistically assess the differences in slow wave JIDs between rest and smartphone behavior, we contrasted them with paired t-tests at each electrode using the LIMO-EEG toolbox [Pernet et al., 2011]. This electrode-wise comparison was chosen because direct comparison of NNMF-derived patterns was not feasible, as the number of low-rank components varied across participants. To control for multiple comparisons, we applied spatiotemporal clustering with 1000 bootstraps and an α level of 0.05.

Next, we measured the relationship between consecutive slow wave intervals and the rate of smartphone interactions. This was calculated as the number of touchscreen interactions during intervals K to K+1, divided by the total duration of those intervals. We assigned each rate to a bin in the 2D joint-interval space. If multiple consecutive intervals fell into the same bin, we added up the total number of interactions and the total duration, then calculated the rate by dividing one by the other. The rate of smartphone interactions was estimated for each participant and electrode. To show population-level patterns, we estimated the median interaction rates across participants for each electrode. To capture a potential delayed relationship between consecutive slow waves and smartphone interactions, we estimated the median time (latency) to the next touchscreen interaction following consecutive slow wave intervals. When visualizing slow waves over time, we observed a trend of increased slow waves during the short pauses before participants switched between apps. To rule out the influence of these breaks, we repeated the analyses after removing those time periods and found no change in the results.

Finally, we examined whether the features of consecutive slow waves varied depending on their

interval dynamics. For each bin, we calculated the median peak-to-peak amplitude and the median duration of the slow waves that occurred during intervals K to K+1. This allowed us to see how slow wave features changed across different parts of the JID.

Data and code availability

The publication will contain links to the data shared on Dataverse.nl. The data is published 1 month after publication. The code is available on GitHub: https://github.com/CODELABCODELIB/slow_waves_2024.

References

[Andrillon et al., 2021] Andrillon, T., Burns, A., Mackay, T., Windt, J., and Tsuchiya, N. (2021). Predicting lapses of attention with sleep-like slow waves. *Nature Communications*, 12(1):3657.

[Balerna and Ghosh, 2018] Balerna, M. and Ghosh, A. (2018). The details of past actions on a smartphone touchscreen are reflected by intrinsic sensorimotor dynamics. *NPJ digital medicine*, 1(1):4.

[Benali et al., 2011] Benali, A., Trippe, J., Weiler, E., Mix, A., Petrasch-Parwez, E., Girzalsky, W., Eysel, U. T., Erdmann, R., and Funke, K. (2011). Theta-burst transcranial magnetic stimulation alters cortical inhibition. *Journal of Neuroscience*, 31(4):1193–1203.

[Benjamini and Yekutieli, 2001] Benjamini, Y. and Yekutieli, D. (2001). The control of the false discovery rate in multiple testing under dependency. *Annals of statistics*, pages 1165–1188.

[Bernardi et al., 2015] Bernardi, G., Siclari, F., Yu, X., Zennig, C., Bellesi, M., Ricciardi, E., Cirelli, C., Ghilardi, M. F., Pietrini, P., and Tononi, G. (2015). Neural and behavioral correlates of extended training during sleep deprivation in humans: evidence for local, task-specific effects. *Journal of neuroscience*, 35(11):4487–4500.

[Bolognini and Ro, 2010] Bolognini, N. and Ro, T. (2010). Transcranial magnetic stimulation: disrupting neural activity to alter and assess brain function. *Journal of Neuroscience*, 30(29):9647–9650.

[Borbély et al., 1982] Borbély, A. A. et al. (1982). A two process model of sleep regulation. *Hum neurobiol*, 1(3):195–204.

[Borger et al., 2019] Borger, J. N., Huber, R., and Ghosh, A. (2019). Capturing sleep–wake cycles by using day-to-day smartphone touchscreen interactions. *NPJ digital medicine*, 2(1):73.

[Brennan et al., 2002] Brennan, M., Palaniswami, M., and Kamen, P. (2002). Do existing measures of poincare plot geometry reflect nonlinear features of heart rate variability? *IEEE transactions on biomedical engineering*, 48(11):1342–1347.

[Cash et al., 2010] Cash, R., Ziemann, U., Murray, K., and Thickbroom, G. W. (2010). Late cortical disinhibition in human motor cortex: a triple-pulse transcranial magnetic stimulation study. *Journal of Neurophysiology*, 103(1):511–518.

[Ceolini and Ghosh, 2023] Ceolini, E. and Ghosh, A. (2023). Common multi-day rhythms in smartphone behavior. *NPJ Digital Medicine*, 6(1):49.

[Ceolini et al., 2022] Ceolini, E., Kock, R., Band, G. P., Stoet, G., and Ghosh, A. (2022). Temporal clusters of age-related behavioral alterations captured in smartphone touchscreen interactions. *Iscience*, 25(8).

[Chauvette et al., 2011] Chauvette, S., Crochet, S., Volgushev, M., and Timofeev, I. (2011). Properties of slow oscillation during slow-wave sleep and anesthesia in cats. *Journal of Neuroscience*, 31(42):14998–15008.

[Crochet et al., 2005] Crochet, S., Chauvette, S., Boucetta, S., and Timofeev, I. (2005). Modulation of synaptic transmission in neocortex by network activities. *European Journal of Neuroscience*, 21(4):1030–1044.

[Delorme and Makeig, 2004] Delorme, A. and Makeig, S. (2004). Eeglab: an open source toolbox for analysis of single-trial eeg dynamics including independent component analysis. *Journal of neuroscience methods*, 134(1):9–21.

[Diekelmann and Born, 2010] Diekelmann, S. and Born, J. (2010). The memory function of sleep. *Nature reviews neuroscience*, 11(2):114–126.

[Duckrow et al., 2021] Duckrow, R. B., Ceolini, E., Zaveri, H. P., Brooks, C., and Ghosh, A. (2021). Artificial neural network trained on smartphone behavior can trace epileptiform activity in epilepsy. *IScience*, 24(6).

[Eagan and Partridge, 1989] Eagan, K. P. and Partridge, L. D. (1989). The sequential-interval state space: a means of displaying temporal information in neuron firing. *Journal of neuroscience methods*, 27(3):245–252.

[Espenhahn et al., 2020] Espenhahn, S., Yan, T., Beltrano, W., Kaur, S., Godfrey, K., Cortese, F., Bray, S., and Harris, A. D. (2020). The effect of movie-watching on electroencephalographic responses to tactile stimulation. *Neuroimage*, 220:117130.

[Ferreri et al., 2011] Ferreri, F., Pasqualetti, P., Määttä, S., Ponzo, D., Ferrarelli, F., Tononi, G., Mervaala, E., Miniussi, C., and Rossini, P. M. (2011). Human brain connectivity during single and paired pulse transcranial magnetic stimulation. *Neuroimage*, 54(1):90–102.

[Finelli et al., 2000] Finelli, L., Baumann, H., Borbély, A., and Achermann, P. (2000). Dual electroencephalogram markers of human sleep homeostasis: correlation between theta activity in waking and slow-wave activity in sleep. *Neuroscience*, 101(3):523–529.

[Gindrat et al., 2015] Gindrat, A.-D., Chytiris, M., Balerna, M., Rouiller, E. M., and Ghosh, A. (2015). Use-dependent cortical processing from fingertips in touchscreen phone users. *Current Biology*, 25(1):109–116.

[Halász et al., 2014] Halász, P., Bódizs, R., Parrino, L., and Terzano, M. (2014). Two features of sleep slow waves: homeostatic and reactive aspects–from long term to instant sleep homeostasis. *Sleep medicine*, 15(10):1184–1195.

[Hinard et al., 2012] Hinard, V., Mikhail, C., Pradervand, S., Curie, T., Houtkooper, R. H., Auwerx, J., Franken, P., and Tafti, M. (2012). Key electrophysiological, molecular, and metabolic signatures of sleep and wakefulness revealed in primary cortical cultures. *Journal of Neuroscience*, 32(36):12506–12517.

[Histed et al., 2009] Histed, M. H., Pasupathy, A., and Miller, E. K. (2009). Learning substrates in the primate prefrontal cortex and striatum: sustained activity related to successful actions. *Neuron*, 63(2):244–253.

[Huber et al., 2004] Huber, R., Felice Ghilardi, M., Massimini, M., and Tononi, G. (2004). Local sleep and learning. *Nature*, 430(6995):78–81.

[Huber et al., 2006] Huber, R., Ghilardi, M. F., Massimini, M., Ferrarelli, F., Riedner, B. A., Peterson, M. J., and Tononi, G. (2006). Arm immobilization causes cortical plastic changes and locally decreases sleep slow wave activity. *Nature neuroscience*, 9(9):1169–1176.

[Huk et al., 2018] Huk, A., Bonnen, K., and He, B. J. (2018). Beyond trial-based paradigms: Continuous behavior, ongoing neural activity, and natural stimuli. *Journal of Neuroscience*, 38(35):7551–7558.

[Hung et al., 2013] Hung, C.-S., Sarasso, S., Ferrarelli, F., Riedner, B., Ghilardi, M. F., Cirelli, C., and Tononi, G. (2013). Local experience-dependent changes in the wake eeg after prolonged wakefulness. *Sleep*, 36(1):59–72.

[Jaramillo et al., 2020] Jaramillo, V., Volk, C., Maric, A., Furrer, M., Fattinger, S., Kurth, S., Lustenberger, C., and Huber, R. (2020). Characterization of overnight slow-wave slope changes across development in an age-, amplitude-, and region-dependent manner. *Sleep*, 43(9):zsaa038.

[Kock et al., 2023] Kock, R., Ceolini, E., Groenewegen, L., and Ghosh, A. (2023). Neural processing of goal and non-goal-directed movements on the smartphone. *Neuroimage: Reports*, 3(2):100164.

[Krueger and Roy, 2016] Krueger, J. M. and Roy, S. (2016). Sleep's kernel: Surprisingly small sections of brain, and even neuronal and glial networks in a dish, display many electrical indicators of sleep. *Scientist (Philadelphia, Pa.)*, 30(3):36.

[Lisboa et al., 2013] Lisboa, P. J., Etchells, T. A., Jarman, I. H., and Chambers, S. J. (2013). Finding reproducible cluster partitions for the k-means algorithm. *BMC bioinformatics*, 14(Suppl 1):S8.

[Luber et al., 2007] Luber, B., Kinnunen, L. H., Rakitin, B. C., Ellsasser, R., Stern, Y., and Lisanby, S. H. (2007). Facilitation of performance in a working memory task with rtms stimulation of the precuneus: frequency-and time-dependent effects. *Brain research*, 1128:120–129.

[Luber and Lisanby, 2014] Luber, B. and Lisanby, S. H. (2014). Enhancement of human cognitive performance using transcranial magnetic stimulation (tms). *Neuroimage*, 85:961–970.

[Massar et al., 2021] Massar, S. A., Chua, X. Y., Soon, C. S., Ng, A. S., Ong, J. L., Chee, N. I., Lee, T. S., Ghosh, A., and Chee, M. W. (2021). Trait-like nocturnal sleep behavior identified by combining wearable, phone-use, and self-report data. *NPJ digital medicine*, 4(1):90.

[Massimini et al., 2024] Massimini, M., Corbetta, M., Sanchez-Vives, M. V., Andrillon, T., Deco, G., Rosanova, M., and Sarasso, S. (2024). Sleep-like cortical dynamics during wakefulness and their network effects following brain injury. *Nature Communications*, 15(1):7207.

[Massimini et al., 2005] Massimini, M., Ferrarelli, F., Huber, R., Esser, S. K., Singh, H., and Tononi, G. (2005). Breakdown of cortical effective connectivity during sleep. *Science*, 309(5744):2228–2232.

[Meer et al., 2020] Meer, J. N. v. d., Breakspear, M., Chang, L. J., Sonkusare, S., and Cocchi, L. (2020). Movie viewing elicits rich and reliable brain state dynamics. *Nature communications*, 11(1):5004.

[Nir et al., 2017] Nir, Y., Andrillon, T., Marmelshtein, A., Suthana, N., Cirelli, C., Tononi, G., and Fried, I. (2017). Selective neuronal lapses precede human cognitive lapses following sleep deprivation. *Nature medicine*, 23(12):1474–1480.

[Pernet et al., 2011] Pernet, C. R., Chauveau, N., Gaspar, C., and Rousselet, G. A. (2011). Limo eeg: a toolbox for hierarchical linear modeling of electroencephalographic data. *Computational intelligence and neuroscience*, 2011(1):831409.

[Pinggal et al., 2022] Pinggal, E., Dockree, P. M., O'Connell, R. G., Bellgrove, M. A., and Andrillon, T. (2022). Pharmacological manipulations of physiological arousal and sleep-like slow waves modulate sustained attention. *Journal of Neuroscience*, 42(43):8113–8124.

[Quercia et al., 2018] Quercia, A., Zappasodi, F., Committeri, G., and Ferrara, M. (2018). Local use-dependent sleep in wakefulness links performance errors to learning. *Frontiers in Human Neuroscience*, 12:122.

[Riedner et al., 2007] Riedner, B. A., Vyazovskiy, V. V., Huber, R., Massimini, M., Esser, S., Murphy, M., and Tononi, G. (2007). Sleep homeostasis and cortical synchronization: Iii. a high-density eeg study of sleep slow waves in humans. *Sleep*, 30(12):1643–1657.

[Rodieck et al., 1962] Rodieck, R. W., Kiang, N.-S., and Gerstein, G. L. (1962). Some quantitative methods for the study of spontaneous activity of single neurons. *Biophysical journal*, 2(4):351–368.

[Sachdev et al., 2015] Sachdev, R. N., Gaspard, N., Gerrard, J. L., Hirsch, L. J., Spencer, D. D., and Zaveri, H. P. (2015). Delta rhythm in wakefulness: evidence from intracranial recordings in human beings. *Journal of neurophysiology*, 114(2):1248–1254.

[Snipes et al., 2022] Snipes, S., Krugliakova, E., Meier, E., and Huber, R. (2022). The theta paradox: 4-8 hz eeg oscillations reflect both sleep pressure and cognitive control. *Journal of Neuroscience*, 42(45):8569–8586.

[Snipes et al., 2023] Snipes, S., Meier, E., Meissner, S., Landolt, H.-P., and Huber, R. (2023). Theta and alpha eeg oscillations reflect sleep need—except during the wake maintenance zone. *bioRxiv*, pages 2023–02.

[Steriade et al., 1993] Steriade, M., McCormick, D. A., and Sejnowski, T. J. (1993). Thalamocortical oscillations in the sleeping and aroused brain. *Science*, 262(5134):679–685.

[Tononi and Cirelli, 2006] Tononi, G. and Cirelli, C. (2006). Sleep function and synaptic homeostasis. *Sleep medicine reviews*, 10(1):49–62.

[van de Ruit and Ghosh, 2022] van de Ruit, M. and Ghosh, A. (2022). Can you hear me now? momentary increase in smartphone usage enhances neural processing of task-irrelevant sound tones. *Neuroimage: Reports*, 2(4):100131.

[van Nieuw Amerongen et al., 2024] van Nieuw Amerongen, A. R., Meppelink, A. M., Ghosh, A., and Thijs, R. D. (2024). Real-world smartphone data can trace the behavioural impact of epilepsy: A case study. *European Journal of Neurology*, 31(12):e16433.

[Vyazovskiy and Harris, 2013] Vyazovskiy, V. V. and Harris, K. D. (2013). Sleep and the single neuron: the role of global slow oscillations in individual cell rest. *Nature Reviews Neuroscience*, 14(6):443–451.

[Vyazovskiy et al., 2013] Vyazovskiy, V. V., Olcese, U., Cirelli, C., and Tononi, G. (2013). Prolonged wakefulness alters neuronal responsiveness to local electrical stimulation of the neocortex in awake rats. *Journal of Sleep Research*, 22(3):239–250.

[Vyazovskiy et al., 2011] Vyazovskiy, V. V., Olcese, U., Hanlon, E. C., Nir, Y., Cirelli, C., and Tononi, G. (2011). Local sleep in awake rats. *Nature*, 472(7344):443–447.

[Wan and Ghosh, 2025] Wan, W. and Ghosh, A. (2025). Fine-grained alignment of cortical signals to smartphone touchscreen temporal pattern. *bioRxiv*, pages 2025–06.

[Wei et al., 2020] Wei, Y., Krishnan, G. P., Marshall, L., Martinetz, T., and Bazhenov, M. (2020). Stimulation augments spike sequence replay and memory consolidation during slow-wave sleep. *Journal of Neuroscience*, 40(4):811–824.

[Xie et al., 2013] Xie, L., Kang, H., Xu, Q., Chen, M. J., Liao, Y., Thiyagarajan, M., O'Donnell, J., Christensen, D. J., Nicholson, C., Iliff, J. J., et al. (2013). Sleep drives metabolite clearance from the adult brain. *science*, 342(6156):373–377.

5 Legends

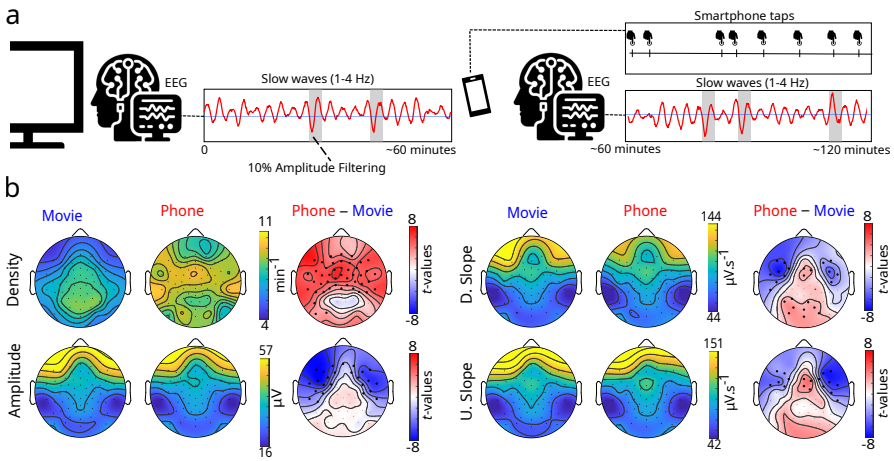

Figure 1. Slow waves were observed during movie watching and smartphone behavior. (a) Schematic overview of the experimental protocol: participants underwent ∼60 minutes of restful movie watching followed by ∼60 minutes of smartphone use, during which slow waves were captured with EEG. **(b)** We contrasted slow wave features between smartphone behavior and restful movie watching using mass-univariate paired t-tests. Scalp topographies display population-average slow wave features: density (slow waves per minute), peak-to-peak amplitude, and downward/upward slopes. For each feature, the left topography shows the mean during rest, the middle topography shows the mean during smartphone behavior, and the right topography shows t-values from the paired t-tests. Statistical significance was assessed with multiple comparison correction in the form of cluster-based permutation testing ($\alpha = 0.05$; 1000 randomizations). Electrodes showing statistically significant differences are marked with black dots on the topographical t-value maps. Slow wave density was higher during smartphone behavior across most of the scalp, except for parieto-occipital regions. In contrast, amplitude was larger at rest, particularly over frontotemporal regions. Both downward and upward slopes were steeper at rest in frontotemporal areas, but shallower in central/occipital regions.

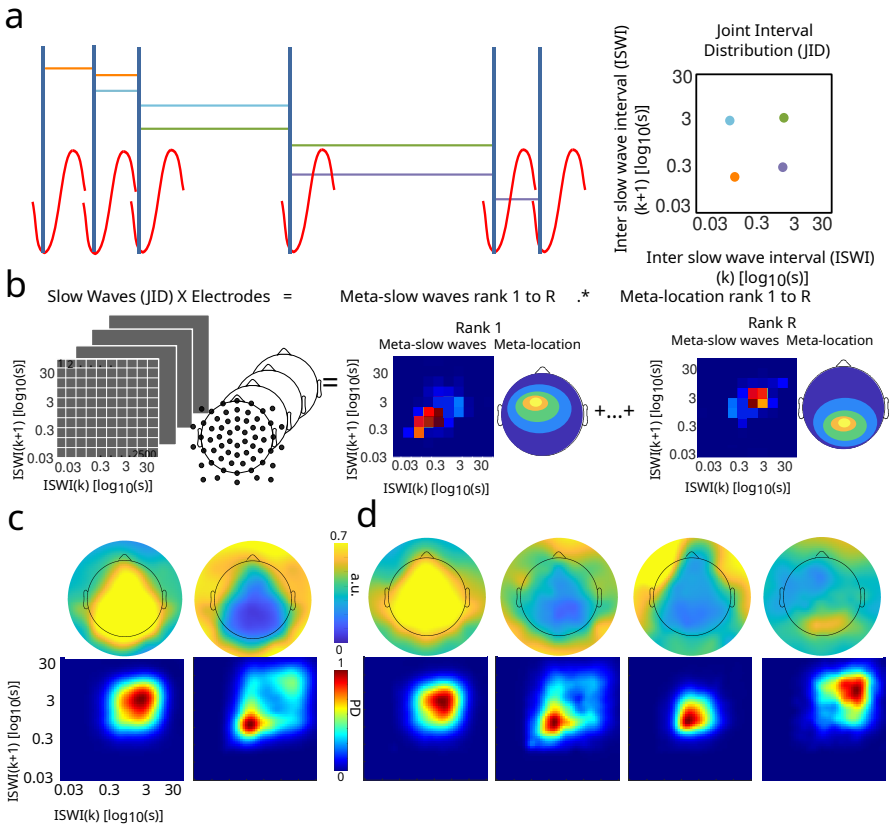

Figure 2. Fine-grained temporal dynamics of slow waves across the population. (a) Method schematic describes how the interval between two consecutive slow wave off-states (K) can be considered along with the next interval ($K+1$). The probabilities of the intervals are pooled in two-dimensional bins, resulting in the joint-interval distribution (JID). **(b)** Schematic showing how the temporal dynamics of slow waves and their spatial locations can be derived using non-negative matrix factorization (NNMF). For each participant, NNMF decomposes a matrix of slow wave JIDs per electrode into low-rank representations: meta-JIDs capturing the typical slow wave dynamics, and meta-locations indicating where these dynamics typically occur on the scalp. **(c)** We clustered the meta-JIDs derived for restful movie watching across the population using k-means, and display the population-level cluster centroids. Scalp topographies show the average (20% trimmed mean) meta-location for each cluster. We identified two clusters: (i) bursts of slow waves are typical in frontal areas, (ii) sparse consecutive slow waves are typical in central and occipital areas. The dynamics are shown in log_{10} space. **(d)** The same analysis was performed for smartphone use, where four clusters were identified: (i) sparse consecutive slow waves across central, parietal, and occipital electrodes, resembling rest; (ii) bursts of consecutive waves with irregular scalp distribution; (iii) moderately rapid consecutive waves mainly in frontal areas; and (iv) sparse consecutive slow waves localized in occipital areas.

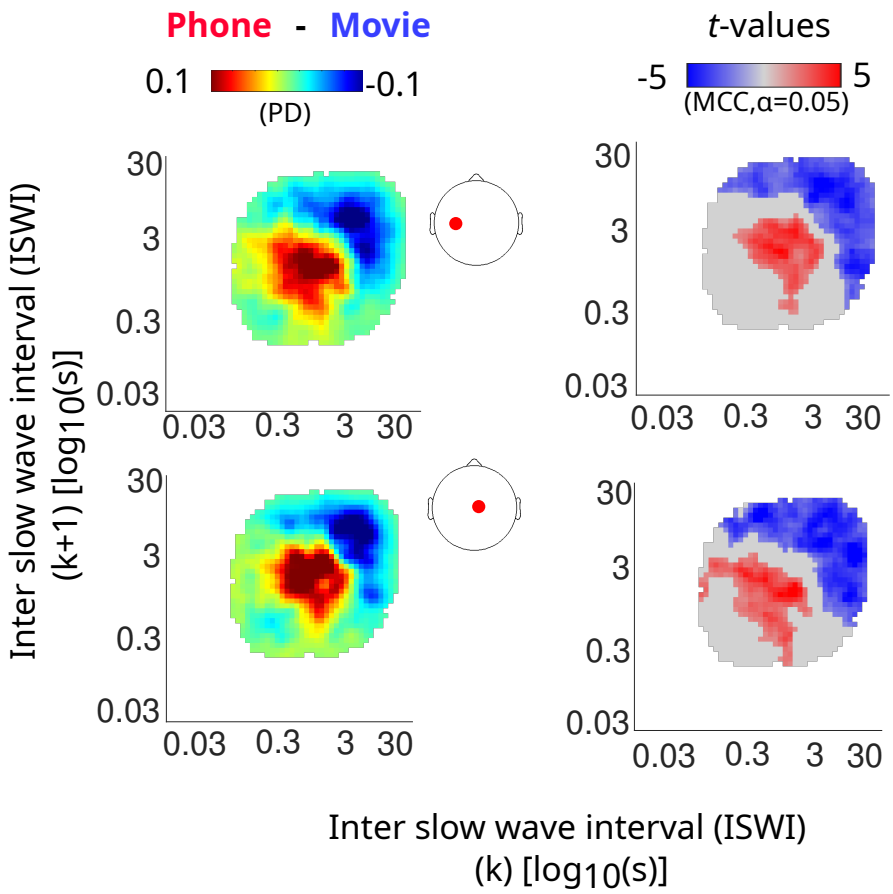

Figure 3. Comparison of slow wave JIDs between restful movie watching and smartphone behavior for representative electrodes (red dots) at the central and sensorimotor areas. Paired t-tests showed that smartphone behavior was accompanied by rapid bursts of slow waves, while at rest, slow waves appeared sparser. Mean differences between slow waves JIDs (smartphone behavior - restful movie watching) are shown in the left column. Statistically significant t-values are displayed in the right column. Statistical significance was assessed using spatiotemporal clustering with multiple comparison correction (MCC), as implemented in LIMO EEG ($\alpha = 0.05$, 1000 bootstraps). Grey indicates no statistically significant clusters and white areas indicate bins with no detected events. PD = probability density.

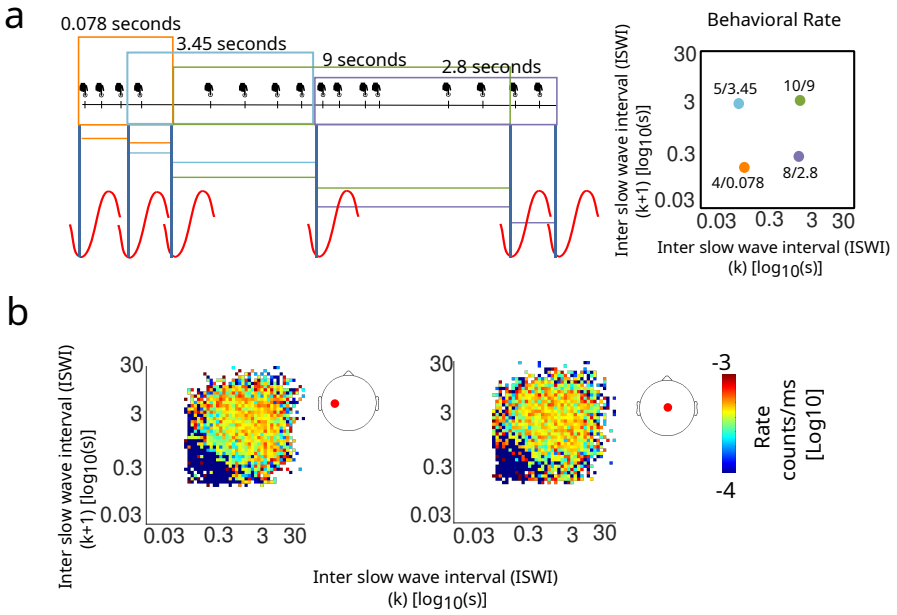

Figure 4. Behavioral rate across slow wave JIDs (a) Schematic illustration of how the rate of smartphone interactions was calculated as the number of smartphone interactions occurring across consecutive slow wave intervals, divided by the total duration of those intervals. **(b)** Rates of interactions were pooled across the population using the median. Representative electrodes (red dots) at the central and sensorimotor areas showed a gradient where the rate of smartphone interactions was lower during rapid consecutive slow waves (i.e., bursts) and higher during sparser consecutive slow waves. White areas indicate bins with no detected events.

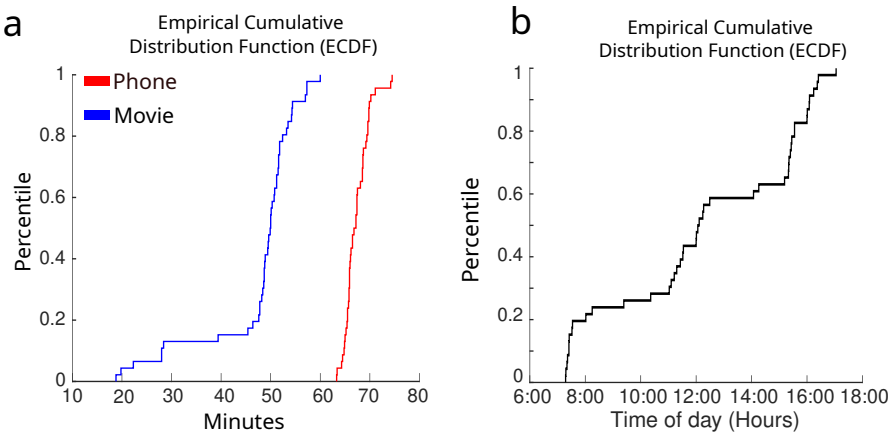

Supplementary Figure 1. Recording times and session start times. (a) Empirical cumulative distribution function (ECDF) of recording times during restful movie watching (blue) and smartphone behavior (red). **(b)** ECDF of the time of day when participants started their measurements.

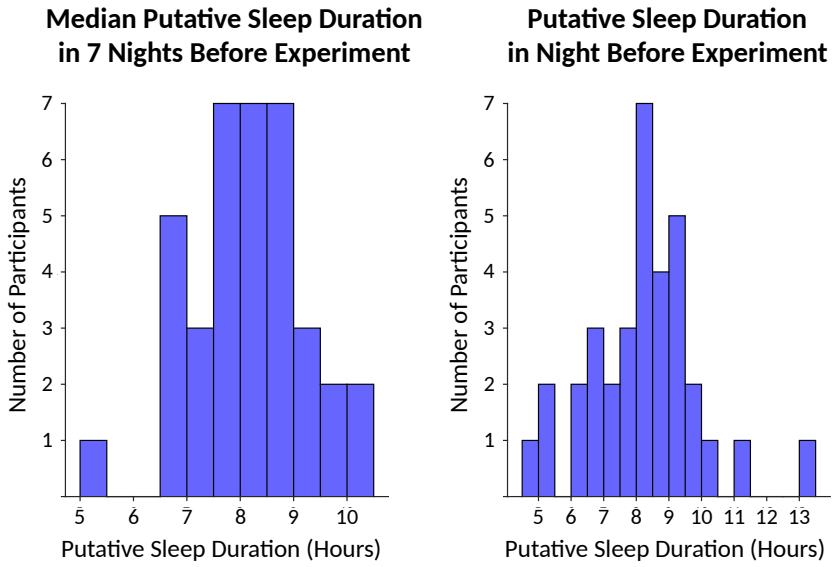

Supplementary Figure 2. Putative sleep durations prior to the measurement. (a) Sleep duration on the night before the measurement, estimated from smartphone usage patterns. The distribution suggests that participants were not experiencing extreme sleep deprivation. **(b)** Median sleep duration across the week before the experiment, also estimated from smartphone data, similarly shows no extreme sleep deprivation. Two participants were excluded from these figures due to missing prior sleep data.

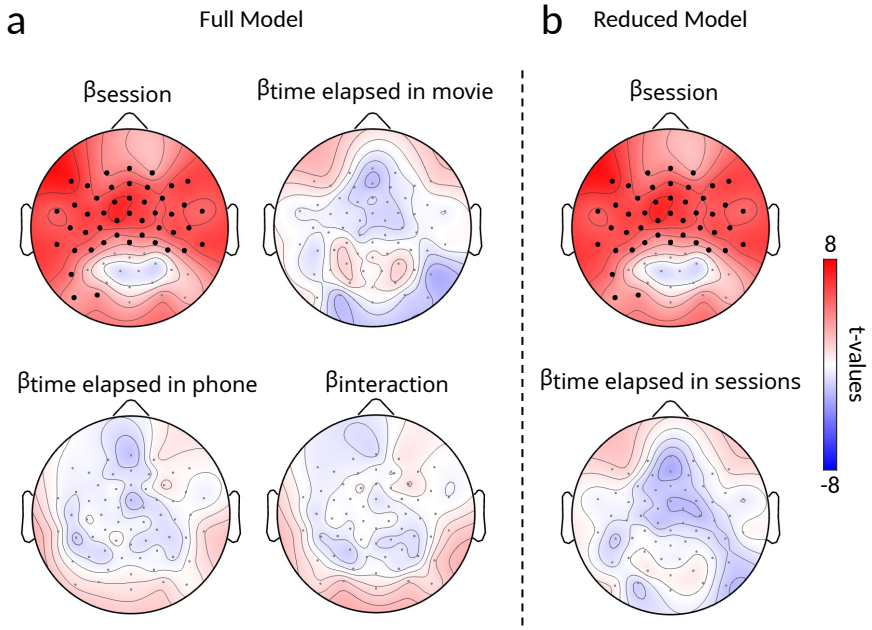

Supplementary Figure 3. Temporal stability of slow wave density across sessions. (a) A mass-univariate linear regression was used to test whether slow wave density (number of slow waves per 1-minute bin) changed over time. Topographical plots denote t-values for the independent variables: (i) session type (restful movie watching or smartphone use), time elapsed within (ii) restful movie watching and (iii) smartphone use sessions, and (iv) the interaction of the two variables. Statistical significance was assessed with multiple comparison correction in the form of cluster-based permutation testing ($\alpha = 0.05$; 1000 randomizations). Only the session type had statistically significant electrodes (black dots), indicating that the number of slow waves changed as a function of behavioral context (smartphone use or rest) but not as a function of time elapsed. **(b)** This analysis was repeated for a reduced model without the interaction term. Again, the effect of time elapsed did not reveal any significant electrode clusters.

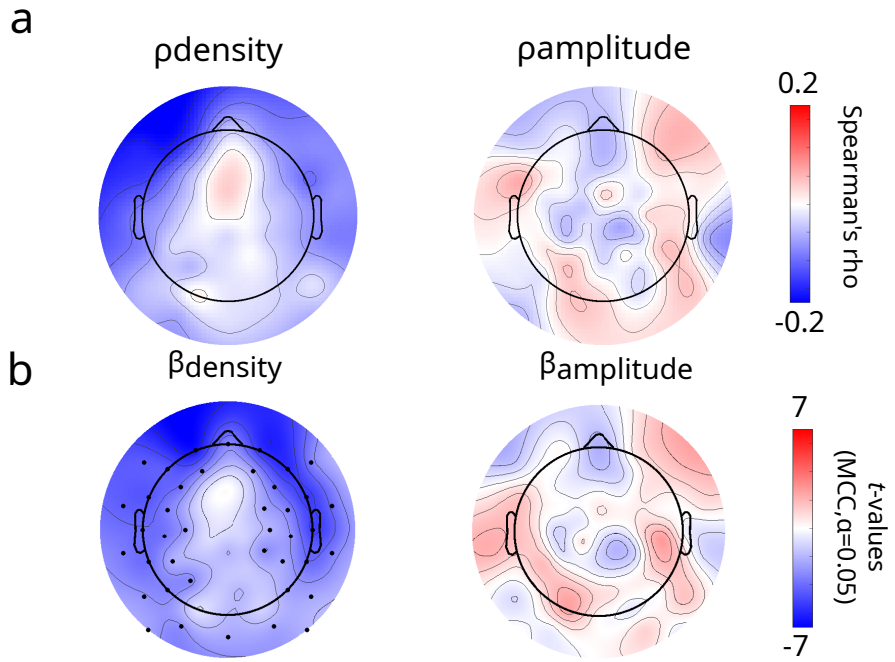

Supplementary Figure 4. Coarse-grained relationship between slow wave features and smartphone interactions. (a) Topographical maps show population-average Spearman's ρ values between the number of smartphone interactions and slow wave density (left) or slow wave amplitude (right), computed within corresponding 1-minute time bins. No reproducible statistically significant correlations were found across the population. **(b)** Hierarchical mass-univariate regressions were performed to test whether slow wave features predict the number of smartphone interactions within corresponding 1-minute time bins. Topographical maps show t-values for slow wave density (left) and slow wave amplitude (right). Statistically significant clusters (black dots) emerged primarily over frontotemporal and sensorimotor regions, where higher slow wave density was associated with fewer smartphone interactions. Statistical significance was assessed using spatiotemporal clustering with multiple comparison correction, as implemented in LIMO EEG ($\alpha = 0.05$, 1000 bootstraps).

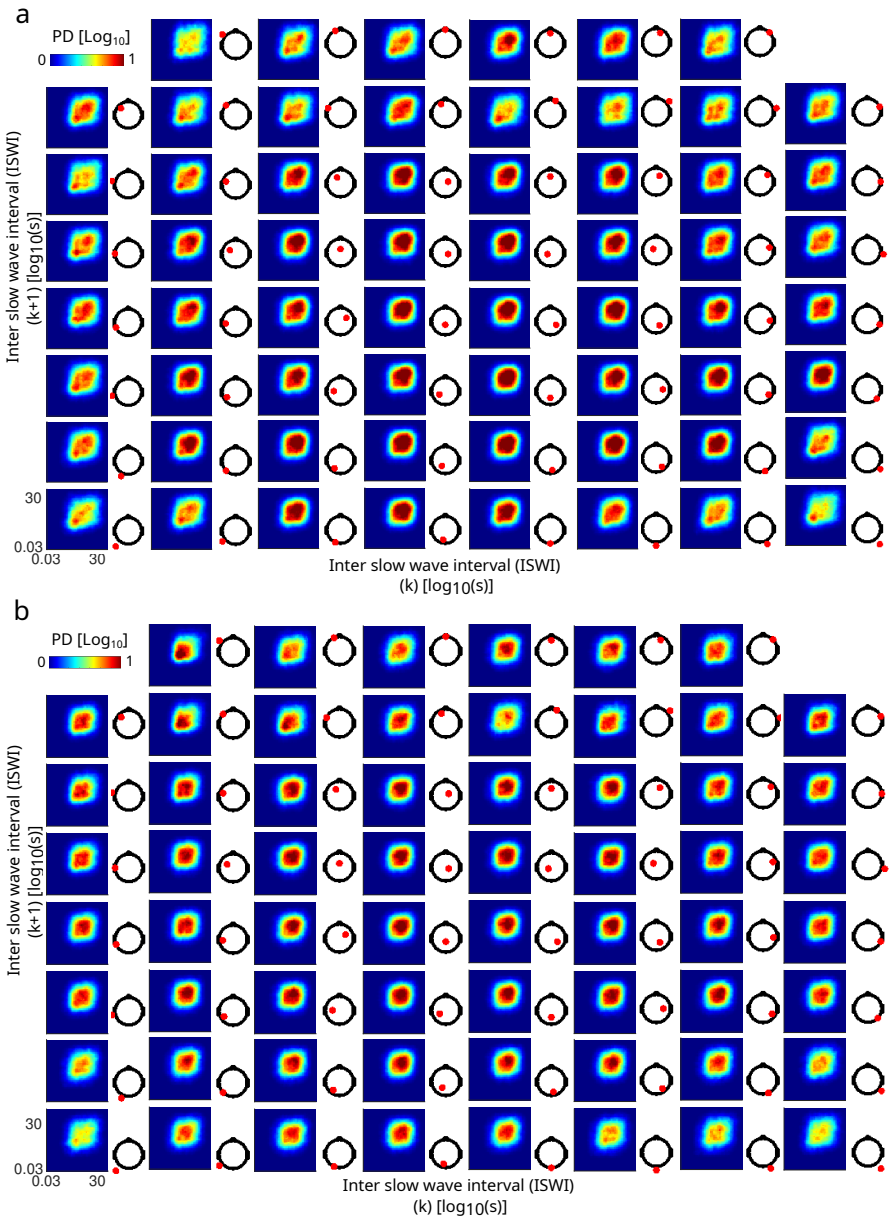

Supplementary Figure 5. Slow wave joint-interval distributions (JIDs) across the population for all electrodes. (a) JIDs during restful movie watching, pooled across participants using the median. Distributions are shown in log_{10} scale. Electrode locations are marked with red dots. **(b)** Same as (a), but for JIDs during smartphone behavior. PD = probability density.

Supplementary Figure 6. Comparison of slow wave JIDs between movie watching and smartphone behavior across all electrodes. We performed paired t-tests between the two sessions. Mean differences between slow wave JIDs (smartphone behavior – restful movie watching) are shown in the left column. Statistically significant t-values are displayed in the middle column. Electrode locations (marked with red dots) are displayed in the right column. Statistical significance was assessed using spatiotemporal clustering with multiple comparison correction, as implemented in LIMO EEG ($\alpha = 0.05$, 1000 bootstraps). Grey indicates no statistically significant clusters, and white indicates that there were no events in the bins. PD = probability density.

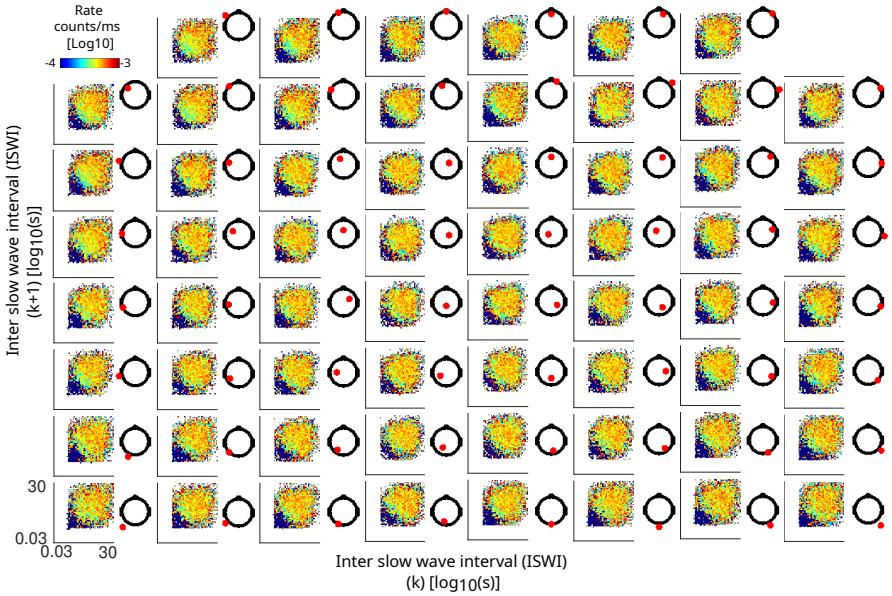

Supplementary Figure 7. Population-level medians for behavioral rate across slow wave JIDs for all scalp electrodes (red dots denote electrode location). The rate of smartphone interactions was lower during rapid bursts of slow waves and higher during sparser consecutive slow waves. The pattern only marginally varied across the scalp. White areas indicate bins with no detected events.

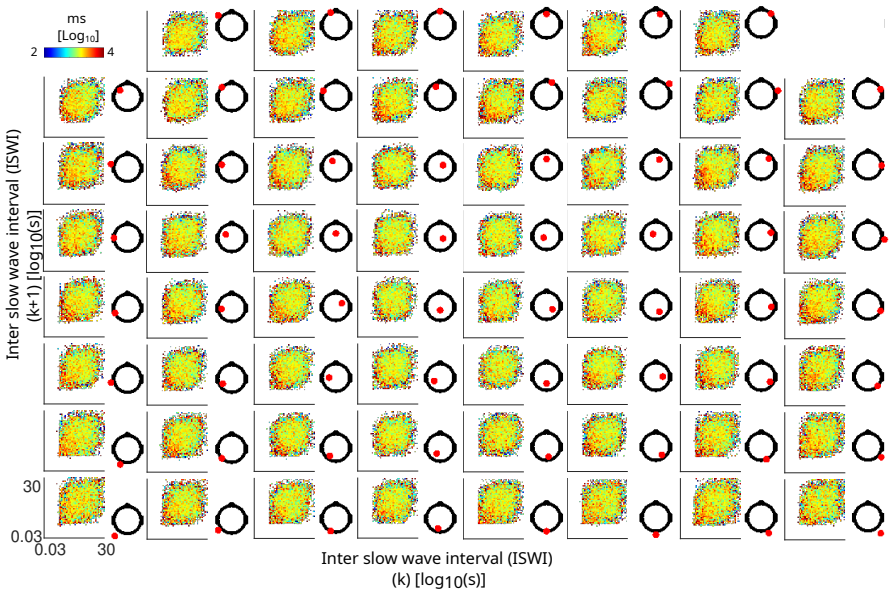

Supplementary Figure 8. Median latency to the next smartphone interaction following consecutive slow waves. A marginal gradient was observed: the next interaction tends to occur later following rapid consecutive slow waves, and sooner following sparse ones. White areas indicate bins with no detected events.

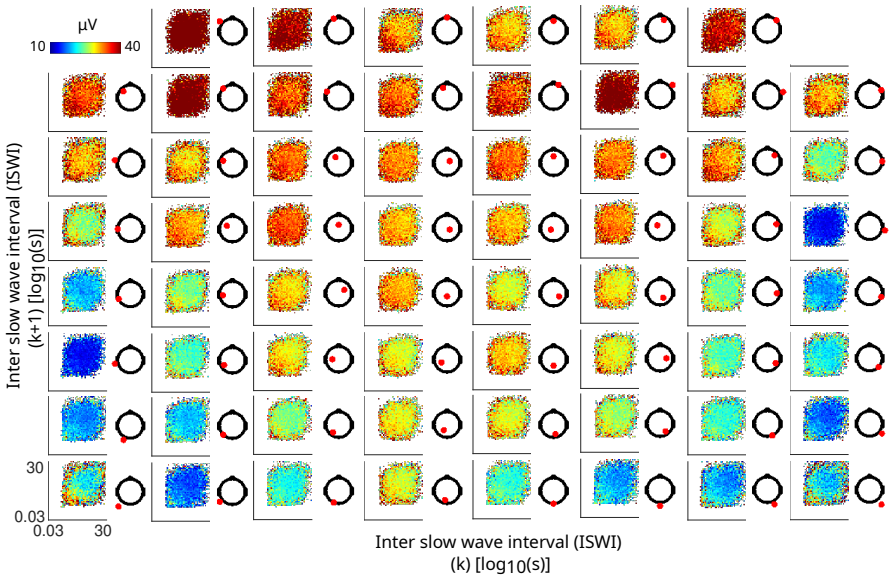

Supplementary Figure 9. Population-level slow wave amplitudes and slopes projected onto the JID. (a) Median peak-to-peak amplitudes were calculated across consecutive slow waves. Amplitudes at each electrode (red dots) were pooled across participants using the median. A gradient along the diagonal showed that the amplitudes decrease as slow waves become sparser. Although this gradient was consistent across electrodes, the average amplitudes varied. White areas indicate bins with no events.

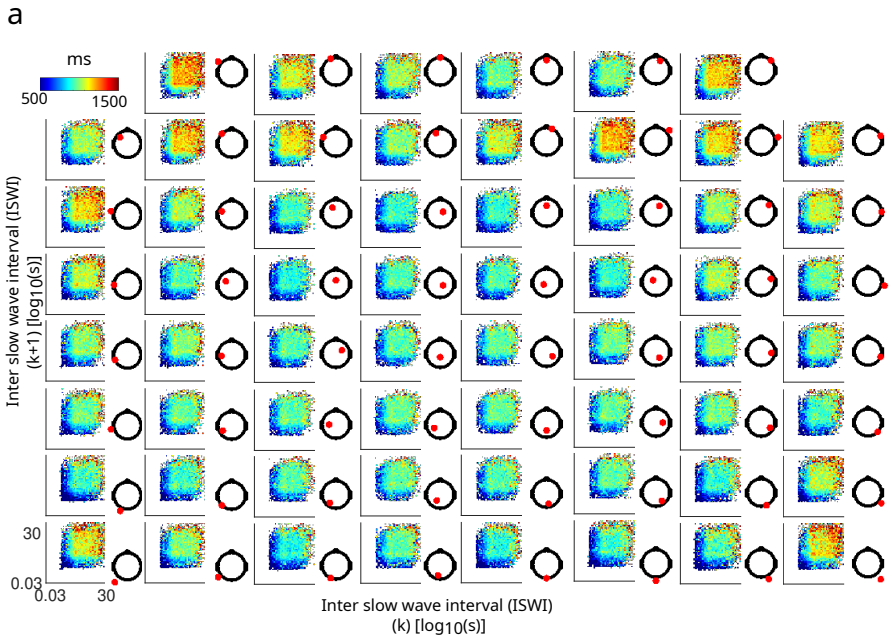

Supplementary Figure 10. Median duration of slow waves (from onset to offset) occurring across consecutive intervals. For each electrode (red dot), we show the resulting median population-level durations projected onto the JID. A gradient emerged: durations were generally shorter during rapid consecutive slow waves and longer during sparse ones. White areas indicate bins with no events.